Spin Hall magnetoresistance in $CoFe_2O_4$/Pt films

Hao Wu[1], Qintong Zhang[1], Caihua Wan[1], Syed Shahbaz Ali[1], Zhonghui Yuan[1], Lu You[2], Junling Wang[2], Yongseong Choi[3], and Xiufeng Han[1,*]

[1]*State Key Laboratory of Magnetism, Beijing National Laboratory of Condensed Matter Physics, Institute of Physics, Chinese Academy of Sciences, Beijing 100190, China*
[2]*School of Materials Science and Engineering, Nanyang Technological University, Singapore 639798, Singapore*
[3]*Advanced Photon Source, Argonne National Laboratory, Argonne, Illinois 60439, USA*

***Abstract*- Pulse laser deposition and magnetron sputtering techniques have been employed to prepare MgO(001)//$CoFe_2O_4$/Pt samples. Cross-section transmission electron microscope confirmed the $CoFe_2O_4$ film epitaxially grew along the (001) direction. X-ray magnetic circular dichroism (XMCD) results show that magnetic proximity effect (MPE) in this sample is negligible. Magnetoresistance (MR) properties confirm that spin hall magnetoresistance (SMR) dominated in this system. Spin Hall effect induced anomalous Hall voltage was also observed in this sample. These results not only demonstrate the universality of SMR effect but also demonstrate the utility in spintronics of $CoFe_2O_4$ as a new type of magnetic insulator.**

***Index Terms*—Spin Hall magnetoresistance, ferrimagnetic insulator, X-ray magnetic circular dichroism, anomalous Hall effect**

I. Introduction

Spintronics is based on both charge and spin degrees of freedom of electrons. Its core content is generating, manipulating and detecting pure spin current [1, 2]. Spin Hall effect [3, 4] and inverse spin Hall effect [5, 6] have been successively discovered and they provide an alternative way to produce and detect pure spin current only by electrical method. Due to its large atomic number and as-induced strong spin orbit coupling energy, platinum (Pt) soon became a competitive candidate in spintronic research.

Recently, Nakayama [7] and Huang [8] even observed anisotropic magnetoresistance (AMR) effect in Pt/YIG system where only Pt contributed to charge transport. AMR [9] is normally observed in magnetic materials and has been widely used in magnetic sensors and data storage. The existence of AMR in a "paramagnetic" material, Pt, though on a ferrimagnetic substrate, soon stimulates a hot debate in community. Huang regarded that the Pt might have been magnetized by the YIG substrate due to magnetic proximity effect (MPE) [8, 10]. In contrast, Nakayama proposed a new mechanism entitled as spin Hall magnetoresistance (SMR) to explain this AMR in Pt/YIG. The key of SMR is the spin current generated by SHE which is then injected into the YIG, and a part of spin current is absorbed by YIG due to the spin transfer torque, while the rest reflected back to Pt, which could enhance the conductivity of Pt. The absorption is maximized or minimized When the magnetization is perpendicular or parallel to $\vec{\sigma}$, therefore the resistance of Pt is affected by the magnetization of YIG [7, 11].

$CoFe_2O_4$ is a ferrimagnetic insulator, and it has a cubic spinel structure. Due to its high saturation magnetization, low coercivity and remanence, small eddy current loss and relatively small conductivity, $CoFe_2O_4$ has been widely used in the field of high frequency devices [12]. In this letter, $CoFe_2O_4$ was used to replace YIG to check the universality of this special MR in ferrimagnetic insulator/Pt system and recheck the possible origins of the unique magnetotransport properties of this system. It is worth noting that the $CoFe_2O_4$ what we used in this research were thin films of nanometer, which were beneficial for future applications compared with its bulk counterparts, so Pt deposited on $CoFe_2O_4$ film [13] is a step towards future applications [14].

II. Experimental Method

In this research work, pulsed laser deposition (PLD) technique has been used to fabricate 30 nm $CoFe_2O_4$ film on MgO (001) substrate with a deposition pressure of 2 Pa and the substrate is heated to 400 °C. The reason for choosing MgO substrate is the low lattice match and similar thermal expansion coefficients of $CoFe_2O_4$ film and MgO substrate. Atomic force microscope (AFM) has been used to scan the surface morphology of $CoFe_2O_4$ film and vibrating sample magnetometer (VSM) has been used to measure the magnetic hysteresis loop of $CoFe_2O_4$ film. The cross-section transmission electron microscopy (TEM) and high resolution TEM (HRTEM) of MgO(001)//$CoFe_2O_4$ interface were observed by Tecnai G2 F20 S-TWIN (200 kV).

A 3 nm Pt layer has been deposited on $CoFe_2O_4$ thin film using ULVAC magnetron sputtering system with a base pressure of 1.0×10^{-6} Pa. Before deposition the surface of $CoFe_2O_4$ film was cleaned by Ar plasma in the preparation chamber and then the sample was transferred to the deposition chamber where 3 nm Pt film at a pressure of 0.16 Pa and a power of 100 W was deposited. Ultraviolet photolithography technique combined with Ar ion beam etching has been used to fabricate Hall bar structure of Pt film. The size of the Hall bar is 100×1000 μm^2. The magnetotransport properties of the samples were measured by physical property measurement system (PPMS). All data was collected at room temperature (300 K).

To check the existence of induced Pt magnetic moment at the $CoFe_2O_4$/Pt interface, we carried out x-ray magnetic circular dichroism (XMCD) measurements. The XMCD measurements were done at Beamline 4-ID-D or the Advanced Photon Source, Argonne National Laboratory. The spectra was collected at the Pt L3 absorption edge (2p→5d transition) to probe the Pt 5d states. The measurements were done in fluorescence mode by collecting the Pt Lα fluorescence intensities with an energy dispersive detector. XMCD was measured by switching helicity of the circularly polarized incident x-ray under a magnetic field of 4 kOe applied along the x-ray propagation direction. To reduce self-absorption effects, the x-ray incident angle was 1° at which the x-ray path within the 3 nm-thick Pt layer is much shorter than the absorption length of the incident x-ray (~2 μm near the Pt L3).

III. Results and Discussion

Fig. 1(a) shows surface morphology of $CoFe_2O_4$ film, the scanned area is 10×10 μm^2 and the roughness is about 0.1 nm, indicating high surface smoothness of the film. Fig. 1(b) shows cross-section HRTEM results of MgO(001)//$CoFe_2O_4$ interface. The results show spinel crystal structure of $CoFe_2O_4$ film was epitaxially formed on the (001) surface of single crystalline MgO substrate after 800 °C high temperature annealing. As shown in the inset image of selected area electron diffraction (SAED), while patterns in red circles come from $CoFe_2O_4$ film, and the rest come from MgO substrate, demonstrating that epitaxial direction of $CoFe_2O_4$ film crystal is along the (001) direction and the lattice parameters is 8.420 Å. Energy Dispersive X-ray Spectroscopy (EDS) of $CoFe_2O_4$ film shows that the atomic ratio of Co and Fe is 1:1.8, close to the ideal ratio of 1:2.

The magnetization of as-deposited $CoFe_2O_4$ film is very small, and it increased significantly after annealing at 800 °C for one hour. The hysteresis loop of in-plane *x* and *y* direction is almost coincidence, as shown in Fig. 2(a), the saturation magnetization M_s, coercive field H_c, saturation field H_s and remanence ratio is 120 emu/cc, 100 Oe, 6000 Oe and 0.13 respectively; and the out of plane H_c, H_s and remanence ratio is 400 Oe, 7000 Oe and 0.24 respectively. The easy axis of magnetization of $CoFe_2O_4$ film tends to align out of plane.

The schematic diagram for magneto-transport measurements is shown in Fig. 2(b), where *x* and *y* directions correspond to the long and short axis of hall bar, *z* direction corresponds to the normal direction of the plane, V_{xx} measures ordinary resistance while V_{xy} measures Hall resistance. The resistance of $CoFe_2O_4$ film itself is larger than 200 MΩ, at least 10^4 times larger than resistance of Pt, thus all the measured electric signals should come from the Pt film.

Fig. 3 shows x-ray absorption spectroscopy (XAS) and XMCD spectra from the 3nm-thick Pt layer sample. An XAS spectrum from a reference Pt foil is similar to the XAS from the sample, indicating the Pt oxidation at the interface is minimal. The XMCD spectrum shows negligible signal at the Pt L3 edge. From the Pt/Co interface, an induced moment of 0.2 μ_B/Pt within the 0.5 nm has been observed [15]. Comparing with these previous results, we estimated the upper limit of the possible XMCD signal in Fig. 3 and it is about two orders of magnitude smaller, indicating that MPE in this MgO(001)//$CoFe_2O_4$/Pt sample is negligible.

It is well established that AMR usually exists in ferromagnetic metals, therefore, in MPE theory Pt is magnetized by $CoFe_2O_4$ and its resistance satisfy $\rho = \rho_\perp + \Delta\rho_A m_x^2$, m_x is the component of magnetization in *x* direction. While according to SMR theory $\rho = \rho_0 - \Delta\rho_s m_y^2$, and m_y is the component of magnetization in *y* direction [11]. In *x* and *y* directions, the signs of MR are the same in both theories, positive in x direction and negative in y direction. However, in *z* direction which is perpendicular to the film, the signs of MR in these two theories are opposite, positive in SMR theory and negative in MPE theory.

The magnetic field range we used in Fig. 4 is large (2 T or 4 T) because the saturation field of $CoFe_2O_4$ film is 6000 Oe (in plane) and 7000 Oe (out of plane). However, it is worth noting that a large field will introduce an ordinary magnetoresistance (OMR) of Pt film, $\rho \propto (\mu B)^2$ to the OMR signals, which should be gotten rid of to acquire a pure MR signal only related to the magnetization of $CoFe_2O_4$.

In our results, the total MR is composed by SMR and OMR. Fig. 4(a) and Fig. 4(b) show total *R*-*H* curves and SMR curves that have been subtracted the OMR contribution of MgO(001)//$CoFe_2O_4$/Pt, and Fig. 4(c) shows *R*-*H* curves of Si//Pt. The magnetic field *H* is along the *x* direction, which is parallel to the current. The OMR under low magnetic field is very small, the MR ratio of Si//Pt is 0.0006 % at 6000 Oe, and 0.0036 % at 4 T. However, we found in MgO(001)//$CoFe_2O_4$/Pt the MR ratio below 6000Oe does not follow the parabolic field dependence, and the MR ratio at 6000 Oe is 0.002 %, whereas at 4 T the MR ratio can reach 0.017 %. Thus the MR data under low magnetic field (⩽6000 Oe) could not be explained by the OMR mechanism. We think that the MR is attributed to SMR mechanism where the resistance increases with *H* as *H* parallel to *I*, and the saturated SMR ratio and magnetic field is respectively 0.002% and 6000 Oe. The critical field 6000 Oe that the SMR is saturated is the same with the saturation field of $CoFe_2O_4$ film measured by VSM.

Fig. 4(d) and Fig. 4(e) show *R*-*H* curves and SMR curves that have been subtracted the OMR contribution of MgO(001)//$CoFe_2O_4$/Pt, and Fig. 4(f) shows *R*-*H* curves of Si//Pt. The magnetic field *H* is applied along the *y* direction, so the directions of current and magnetic field are vertical. At low magnetic field (⩽6000 Oe), we observed that the resistance decreases with increasing magnetic field, and the MR ratio at 6000 Oe is -0.001%, which is consistent with the physical picture of SMR. While at high field (⩾6000 Oe) the resistance increases with the increase in the magnetic field, and the MR ratio at 4 T can reach 0.008%, this unsaturated MR results from the OMR. The SMR and the OMR signals are opposite in sign, so we can easily exclude the possibility that the low field MR comes from the OMR. In contrast, we only observed an OMR in Si//Pt, the MR monotonously increases with field and the MR ratio at 4 T is 0.004%.

Fig. 4(g) and Fig. 4(h) show total *R-H* curves and SMR curves that have been subtracted the OMR contribution of MgO(001)//$CoFe_2O_4$/Pt, and Fig. 4(i) shows *R-H* curves of Si//Pt. The magnetic field *H* is along the *z* direction. After subtracting the OMR contribution, We observed a small positive MR (10^{-6}) in MgO(001)//$CoFe_2O_4$/Pt, as in the x direction, which is in accordance with the SMR theory and contrary to the MPE theory. This signal is very weak because the easy axis of magnetization tends to be along z direction, so the magnetization of $CoFe_2O_4$ didn't change too much by field along z direction. We also observed the OMR in MgO(001)//$CoFe_2O_4$/Pt and Si//Pt samples.

Fig. 5(a) and Fig. 5(b) show the results of Hall effect of MgO(001)//$CoFe_2O_4$/Pt and Si//Pt, the magnetic field *H* is perpendicular to $CoFe_2O_4$ film. In Si//Pt, we can only observe a linear dependence of Hall resistance $\rho_{xy} = R_0 H$, and the slope corresponds to the ordinary Hall coefficient R_0 (-1.22×10^{-13} Ω·cm/Oe). In contrast, we observed an obvious spin Hall effect induced anomalous Hall voltage in MgO(001)//$CoFe_2O_4$/Pt which is related to the magnetization of $CoFe_2O_4$ film. In SMR theory, $\rho_{xy} = \rho_{2,s} m_z + \rho_{3,s} m_x m_y + R_0 H$. The Hall voltage is unsaturated due to the influence of ordinary Hall effect (OHE).

In addition, the *R-H* curves in Fig. 4 are asymmetric between +*H* and –*H*. The *MR* at +*H* is slightly different from that at –*H*. Besides, the minimum of R_{xx} appears not at zero fields but instead, as shown in Fig. 4(c), at -10 kOe. This asymmetry, we think, comes from intermixing between R_{xx} and R_{xy} signals, which is induced by small geometrical asymmetry of Hall bar and/or inhomogeneity in the film thickness of Pt film. The intermixing between R_{xx} and R_{xy} signals also introduce a parabolic component into Hall resistivity as shown in Fig.5 (a), which results in different slopes at +*H* and –*H* in Hall loops.

IV. Conclusion

In conclusion, we observed SMR (~10^{-5}) combining with OMR in MgO(001)//$CoFe_2O_4$/Pt at room temperature, which corresponds to the magnetization of $CoFe_2O_4$. XMCD results show that the induced Pt moment is negligibly small, at least 2 orders of magnitude smaller than in Co/Pt case, indicating that MPE in this sample is negligible. The MR properties in three directions confirm SMR mechanism dominates in this system. Spin Hall effect induced anomalous Hall voltage was also observed in this sample. In contrast, we only observed OMR and OHE in Si//Pt samples. These results not only demonstrate the universality of SMR effect but also demonstrate the utility in spintronics of $CoFe_2O_4$ as a new type of ferrimagnetic insulator.

Acknowledgment

The project was supported by the State Key Project of Fundamental Research and 863 Plan Project of Ministry of Science and Technology [MOST, No. 2010CB934401 and 2014AA032904] and National Natural Science Foundation of China [NSFC, Grant No. 11374351 and 51229101]. Work at the Advanced Photon Source is supported by the US Department of Energy, Office of Science [Grant No. DE-AC02-06CH11357].

References

[1] S. A. Wolf, D. D. Awschalom, R. A. Buhrman, J. M. Daughton, S. V. Molnar, M. L. Roukes, A.Y. Chtchelkanova, and D. M. Treger, "Spintronics: a spin-based electronics vision for the future," Science, vol. 294, p. 1488, Nov. 2001.

[2] I. Žutić, J. Fabian, and S. D. Sarma, "Spintronics: Fundamentals and applications," Rev. Mod. Phys., vol. 76, p. 323, Apr. 2004.

[3] Y. K. Kato, R. C. Myers, A. C. Gossard, and D. D. Awschalom, "Observation of the spin Hall effect in semiconductors," Science, vol. 306, p. 1910, Nov. 2004.

[4] S. O. Valenzuela, and M. Tinkham, "Direct electronic measurement of the spin Hall effect," Nature, vol. 442, p. 176, Jul. 2006.

[5] E. Saitoh, M. Ueda, H. Miyajima, and G. Tatara, "Conversion of spin current into charge current at room temperature: Inverse spin-Hall effect," Appl. Phys. Lett., vol. 88, p. 182509, May. 2006.

[6] T. Kimura, Y. Otani, T. Sato, S. Takahashi, and S. Maekawa, "Room-temperature reversible spin Hall effect," Phys. Rev. Lett., vol. 98, p. 156601, Apr. 2007.

[7] H. Nakayama, M. Althammer, Y. T. Chen, K. Uchida, Y. Kajiwara, D. Kikuchi, T. Ohtani, S. Geprags, M. Opel, S. Takahashi, R. Gross, G. E. W. Bauer, S. T. B. Goennenwein, and E. Saitoh, "Spin Hall magnetoresistance induced by a nonequilibrium proximity effect," Phys. Rev. Lett., vol. 110, p. 206601, May. 2013.

[8] S. Y. Huang, X. Fan, D. Qu, Y. P. Chen, W. G. Wang, J. Wu, T. Y. Chen, J. Q. Xiao, and C. L. Chien, "Transport magnetic proximity effects in platinum," Phys. Rev. Lett., vol. 109, p. 107204, Sep. 2012.

[9] D. A. Thompson, L. T. Romankiw, and A. Mayadas, "Thin film magnetoresistors in memory, storage, and related applications," IEEE Trans. Magn., vol. 11, p. 1039, Jul. 1975.

[10] Y. M. Lu, Y. Choi, C. M. Ortega, X. M. Cheng, J. W. Cai, S. Y. Huang, L. Sun, and C. L. Chien, "Pt Magnetic Polarization on $Y_3Fe_5O_{12}$ and Magnetotransport Characteristics," Phys. Rev. Lett., vol. 110, p. 147207, Apr. 2013.

[11] Y. T. Chen, S. Takahashi, H. Nakayama, M. Althammer, S. T. B. Goennenwein, E. Saitoh, and G. E. W. Bauer, "Theory of spin Hall magnetoresistance," Phys. Rev. B, vol. 87, p. 144411, Apr. 2013.

[12] Q. Song Q, and Z. J. Zhang , "Shape control and associated magnetic properties of spinel cobalt ferrite nanocrystals," J. Am. Chem. Soc., vol. 126, p. 6164, Jan. 2004.

[13] Y. Suzuki, R. G. V. Dover, E. M. Gyorgy, J. M. Phillips, V. Korenivski, D. J. Werder, C. H. Chen, R. J. Cava, J. J. Krajewski, W. F. J. Peck, and K. B. Do, "Structure and magnetic properties of epitaxial spinel ferrite thin films," Appl. Phys. Lett., vol. 68, p. 714, Jan. 1996.

[14] M. Isasa, A. Bedoya-Pinto, S. Velez, F. Golmar, F. Sanchez, L. E. Hueso, J. Fontcuberta, and F. Casanova, "Spin Hall magnetoresistance at Pt/$CoFe_2O_4$ interfaces and texture effects," Appl. Phys. Lett., vol. 105, p. 142402, Oct. 2014.

[15] M. Suzuki, H. Muraoka, Y. Inaba, H. Miyagawa, N. Kawamura, T. Shimatsu, H. Maruyama, N. Ishimatsu, Y. Isohama, and Y. Sonobe, "Depth profile of spin and orbital magnetic moments in a subnanometer Pt film on Co," Phys. Rev. B, vol.72, p. 054430, Aug. 2005.

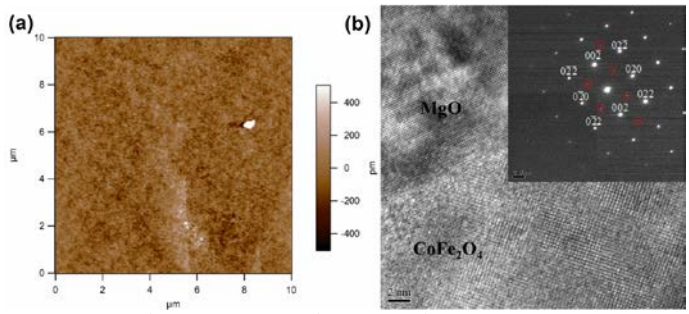

Fig. 1. (a) Surface topography of $CoFe_2O_4$ film. (b) Cross-section high resolution transmission electron microscopy (HRTEM) image and selected area electron diffraction (SAED) patterns of MgO(001)// $CoFe_2O_4$ interface.

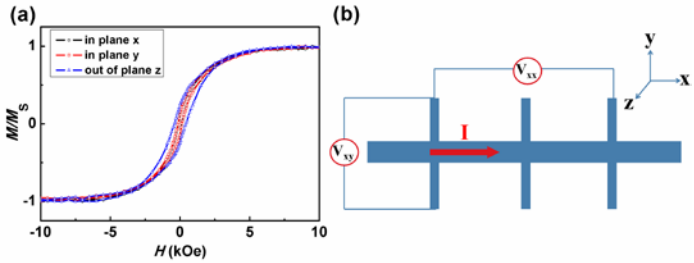

Fig. 2. (a) Magnetic hysteresis loops of the $CoFe_2O_4$ film. (b) Schematic diagram for magnetotransport measurements.

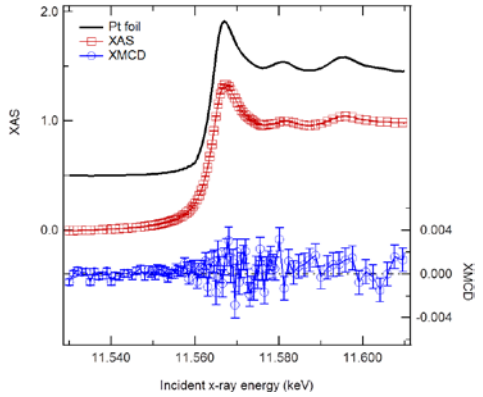

Fig. 3. XAS and XMCD spectra normalized to the Pt L3 edge jump from the MgO(001)//$CoFe_2O_4$/Pt sample. The XAS from a reference Pt is shifted up for clarity.

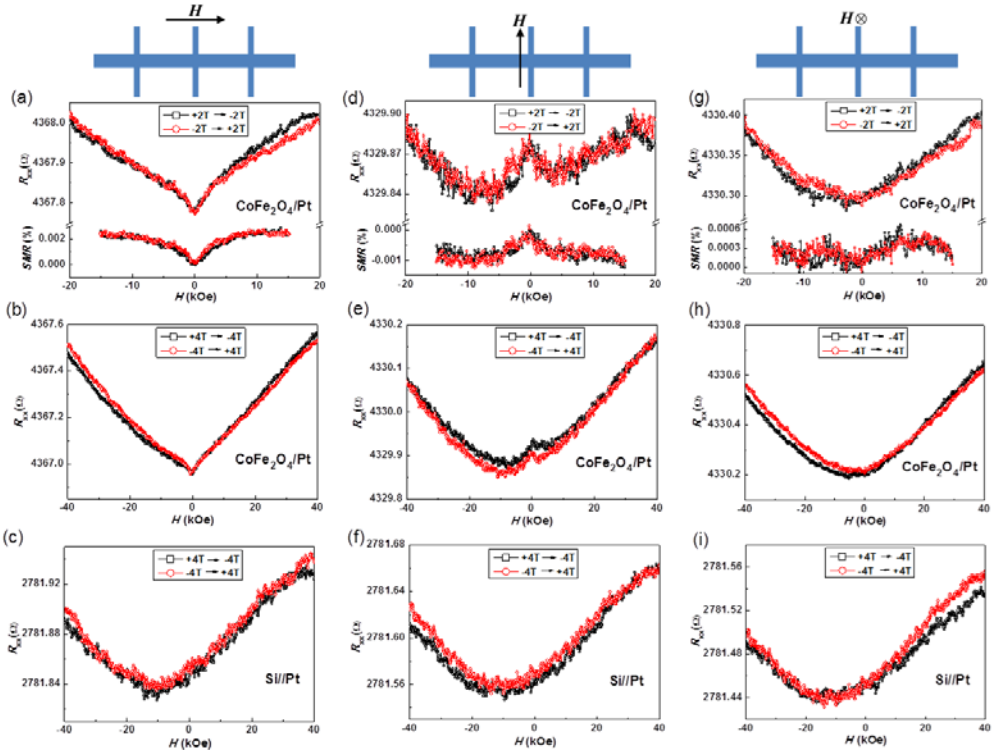

Fig. 4. (a), (b) , (d), (e), (g), (h) 2 T and 4 T *R*-*H* and SMR curves of MgO(001)//$CoFe_2O_4$/Pt in *x*, *y* and *z* directions; (c), (f), (i) 4 T *R*-*H* curves of Si//Pt in *x*, *y* and *z* directions.

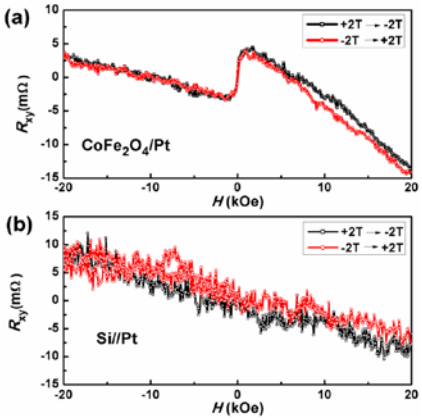

Fig. 5. (a) Anomalous and ordinary Hall resistance of MgO(001)//$CoFe_2O_4$/Pt.
(b) Ordinary Hall resistance of Si//Pt.